JACS
JOURNAL OF THE AMERICAN CHEMICAL SOCIETY

ARTICLE

pubs.acs.org/JACS

Evaluation of Diverse α/β-Backbone Patterns for Functional α-Helix Mimicry: Analogues of the Bim BH3 Domain

Melissa D. Boersma,[†] Holly S. Haase,[†] Kimberly J. Peterson-Kaufman,[†] Erinna F. Lee,[‡,§] Oliver B. Clarke,[‡,§] Peter M. Colman,[‡,§] Brian J. Smith,[‡,§] W. Seth Horne,[†] W. Douglas Fairlie,[*,‡,§] and Samuel H. Gellman[*,†]

[†]Department of Chemistry, University of Wisconsin-Madison, Madison, Wisconsin 53706, United States

[‡]The Walter and Eliza Hall Institute for Medical Research, Parkville, Victoria 3052, Australia

[§]Department of Medical Biology, The University of Melbourne, Parkville, Victoria 3010, Australia

Supporting Information

ABSTRACT: Peptidic oligomers that contain both α- and β-amino acid residues, in regular patterns throughout the backbone, are emerging as structural mimics of α-helix-forming conventional peptides (composed exclusively of α-amino acid residues). Here we describe a comprehensive evaluation of diverse α/β-peptide homologues of the Bim BH3 domain in terms of their ability to bind to the BH3-recognition sites on two partner proteins, Bcl-x_L and Mcl-1. These proteins are members of the anti-apoptotic Bcl-2 family, and both bind tightly to the Bim BH3 domain itself. All α/β-peptide homologues retain the side-chain sequence of the Bim BH3 domain, but each homologue contains periodic α-residue → β^3-residue substitutions. Previous work has shown that the $\alpha\alpha\beta\alpha\alpha\alpha\beta$ pattern, which aligns the β^3-residues in a 'stripe' along one side of the helix, can support functional α-helix mimicry, and the results reported here strengthen this conclusion. The present study provides the first evaluation of functional mimicry by $\alpha\alpha\beta$ and $\alpha\alpha\alpha\beta$ patterns, which cause the β^3-residues to spiral around the helix periphery. We find that the $\alpha\alpha\alpha\beta$ pattern can support effective mimicry of the Bim BH3 domain, as manifested by the crystal structure of an α/β-peptide bound to Bcl-x_L, affinity for a variety of Bcl-2 family proteins, and induction of apoptotic signaling in mouse embryonic fibroblast extracts. The best $\alpha\alpha\alpha\beta$ homologue shows substantial protection from proteolytic degradation relative to the Bim BH3 α-peptide.

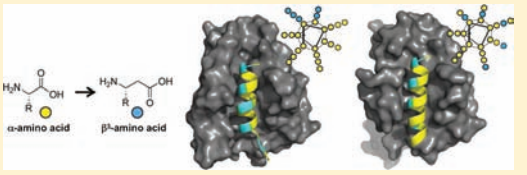

INTRODUCTION

Biological systems frequently encode recognition information in α-helical segments of proteins, to be read out by complementary surfaces on partner proteins.[1] Many groups have explored unnatural oligomers as replacements for the poly-α-amino acid backbone, with the goal of maintaining the three-dimensional arrangements of side chains that make partner contacts while eliminating susceptibility to proteolytic degradation and enhancing conformational stability.[2] A long-term aim of such efforts is to identify design strategies that are broadly applicable to mimicry of diverse α-helical signals. This prospect is encouraged by the regularity of the α-helix itself. Modest structural deviations between the α-helix and an unnatural analogue may be tolerated for mimicry of short helices, but such deviations will become increasingly problematic as length increases. To date, oligomers with purely unnatural backbones (e.g., β-peptides,[3] peptoids,[4] aromatic-rich oligomers[5]) have been evaluated for mimicry of segments containing up to three consecutive α-helical turns; helical protein recognition motifs of this size can be mimicked also via more traditional medicinal chemistry strategies, which focus on small, nonoligomeric molecules.[6] Covalent cross-linking strategies that stabilize α-helical conformations of peptides represent an alternative to unnatural backbones.[7] Recent results with purely hydrocarbon cross-links, between pairs of side chains or between the backbone and a side chain, have been particularly impressive in terms of biological activity.

We have pursued an approach to functional α-helix mimicry that is conceptually related both to the use of purely unnatural backbones and to strategies that retain the natural α-amino acid backbone while introducing unnatural components to confer stability. Our approach is based on modifying a helix-forming sequence by partial replacement of the original α-amino acid residues with analogous β-amino acid residues.[8] If the β^3-residues are distributed throughout the sequence, the resulting α/β-peptides can display substantial resistance to proteolysis[9] while retaining the ability to form an α-helix-like conformation. We have evaluated this strategy for mimicry of an α-helical prototype in two protein-recognition contexts: interaction between a BH3 domain and the complementary cleft on an anti-apoptotic Bcl-2 family protein,[10,11] and interaction between the C-terminal heptad repeat (CHR) segment of HIV protein gp41 and the complementary groove formed by two adjacent N-terminal heptad repeat (NHR) segments of gp41.[12] In both systems, we have achieved success with an $\alpha\alpha\beta\alpha\alpha\alpha\beta$ heptad repeat backbone pattern, which leads to alignment of the β-residues as a 'stripe' along one side of

Received: August 3, 2011
Published: October 31, 2011

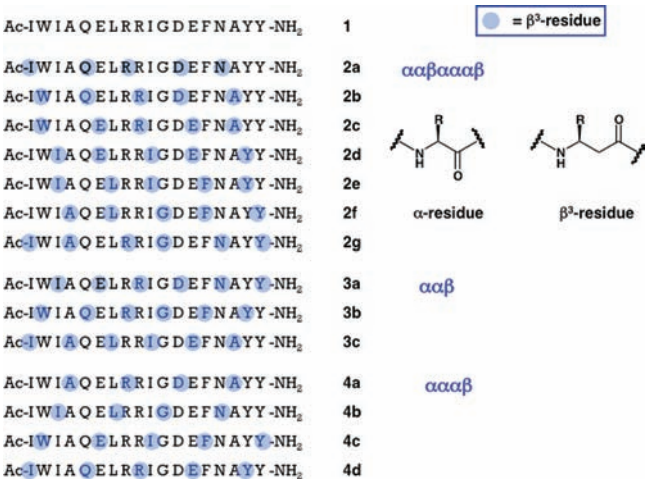

Figure 1. Sequences of 18-mer α-peptide **1**, derived from the Bim BH3 domain, and 18-mer α/β-peptides of families **2**−**4**. The standard single-letter code is used to designate α-amino acid residues. Blue dots are used to indicate the positions of β^3-amino acid residues, which bear the side chain of the α-amino acid residue identified by the single-letter code. Thus, all peptides shown here have the same sequence of side chains, but they have varying backbones (each β^3-residue introduces an additional CH_2 unit relative to the analogous α-residue).

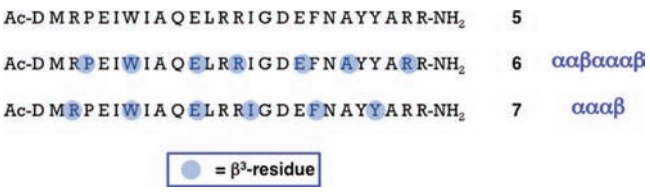

Figure 2. Sequences of 26-mer α-peptide **5**, derived from the Bim BH3 domain, and 26-mer α/β-peptides **6** and **7**, which are extensions of 18-mer α/β-peptides **2c** and **4c**, respectively. The standard single-letter code is used to designate α-amino acid residues. Blue dots are used to indicate the positions of β^3-amino acid residues, which bear the side chain of the α-amino acid residue identified by the single-letter code. Thus, peptides **5**−**7** have the same sequence of side chains, but they have varying backbones (each β^3-residue introduces an additional CH_2 unit relative to the analogous α-residue).

the α/β-peptide helix. This α/β pattern permits the segregation of the unnatural residues to a region of the helical surface that makes minimal contact with the partner protein surface. Here we extend the α/β approach by comprehensively evaluating all possible $\alpha\alpha\beta\alpha\alpha\alpha\beta$, $\alpha\alpha\beta$, and $\alpha\alpha\alpha\beta$ repeat patterns in the context of mimicking the Bim BH3 domain. Previous studies of self-assembling α/β-peptides (derivatives of GCN4-pLI[13]) showed that all three of these α/β patterns can lead to formation of α-helix-like conformations.[8] BH3 domain mimicry serves as a useful testbed for assessment of *functional* α-helix-based design strategies that can subsequently be extended to other, longer systems, as illustrated by our results with gp41 CHR mimicry (10 α-helical turns).[12]

RESULTS AND DISCUSSION

Binding Survey of Diverse *α/β* Patterns. α/β-Peptides **2a**−**g**, **3a**−**c**, and **4a**−**d** share the side-chain sequence of 18-mer α-peptide **1**, which encompasses the core of the Bim BH3 domain plus some flanking residues (Figure 1). Each of these α/β-peptides contains $\alpha \rightarrow \beta^3$ replacements at 5 or 6 of the 18 positions; the β^3-amino acid residues retain the original Bim BH3 side chain but introduce a CH_2 unit between the side-chain-bearing carbon and the carbonyl. Members of family **2** share the $\alpha\alpha\beta\alpha\alpha\alpha\beta$ pattern, and all seven ways in which this pattern can be realized are represented. Family **3** contains all three versions of the $\alpha\alpha\beta$ pattern, and family **4** contains all four versions of the $\alpha\alpha\alpha\beta$ pattern. Prior studies of Bim BH3 have focused on longer peptides (α-residues only), such as 26-mer **5** (Figure 2),[14] but during preliminary experiments we found that 18-mer **1** retains high affinity for the anti-apoptotic protein Mcl-1 and moderate affinity for Bcl-x_L.[15] Starting from a relatively short α-peptide prototype has facilitated our comprehensive evaluation of different α/β patterns because shorter peptides are generally easier to synthesize than longer analogues. This initial survey has allowed us to identify β^3-residue patterns that ultimately proved to be very effective in the 26-mer format.

Figure 3 summarizes the affinities for Mcl-1 and for Bcl-x_L of all possible α/β^3 analogues of the Bim BH3 peptide **1** that have an $\alpha\alpha\beta\alpha\alpha\alpha\beta$, $\alpha\alpha\beta$, or $\alpha\alpha\alpha\beta$ backbone pattern. We focused on Mcl-1 and Bcl-x_L because these two anti-apoptotic proteins are representative of selectivity patterns among BH3 domains within the Bcl-2 family: some BH3 domain peptides (including Bim and Puma) are promiscuous and bind to all anti-apoptotic family members, but others bind to only select subsets.[16] For example, Noxa binds to Mcl-1 but not Bcl-x_L or Bcl-2, while Bad binds to Bcl-x_L and Bcl-2 but not Mcl-1. The K_i data in Figure 3 were obtained via competition fluorescence polarization (FP) assays, in which each α/β-peptide is evaluated for its ability to displace from Bcl-x_L or Mcl-1 a tight-binding, fluorophore-bearing BH3 domain peptide (a Bak-derived 16-mer and a Bim-derived 15-mer, respectively, that have been previously described).[15] One among the $\alpha\alpha\beta\alpha\alpha\alpha\beta$ series approaches **1** in terms of binding to Bcl-x_L ($K_i \approx 23$ nM for **1** vs ~130 nM for **2d**), and one among the $\alpha\alpha\alpha\beta$ series shows slightly improved affinity for this protein ($K_i \approx 50$ nM for **4c**). A single member of the $\alpha\alpha\beta$ series binds detectably to Bcl-x_L ($K_i \approx 520$ nM for **3c**), with affinity 23-fold weaker than was observed for **1**. The results obtained with Mcl-1 were less favorable than those obtained with Bcl-x_L, since none of the 18-mer α/β-peptides approaches the high Mcl-1 affinity observed for the Bim BH3 α-peptide **1** ($K_i < 3$ nM). However, **2c**, **4c** and **4d** displayed moderate affinity for Mcl-1. It is intriguing that some members of the α/β-peptide library display selectivity patterns distinct from that of the Bim BH3 prototype: α-peptide **1** binds ≥10-fold more tightly to Mcl-1 than to Bcl-x_L, but **4c** binds with similar affinities to these two proteins, and **2d** binds ~60-fold more tightly to Bcl-x_L than to Mcl-1.

Co-crystal Structures. We chose **2c** and **4c** among the 18-mer α/β-peptides for further scrutiny because each displayed significant affinity for both of the antiapoptotic proteins employed in the initial binding studies. Each of these α/β-peptides was co-crystallized with Bcl-x_L, and the structures of these complexes were solved to 1.5 Å (**2c**:Bcl-x_L) and 2.5 Å (**4c**:Bcl-x_L) resolution (Supplementary Table 3, Supporting Information [SI] and Figure 4B,C). These new data enable a detailed comparison of the two α/β-peptide:Bcl-x_L structures with the structure of Bim BH3 domain α-peptide **5** bound to Bcl-x_L (PDB: 3FDL; Figure 4A). Bcl-x_L is very similar in all cases, with the exception of helix α3, where differences in the traces of the backbones were observed (Figure 4D). This helix appears to be very flexible in Bcl-x_L and has been shown to adopt different

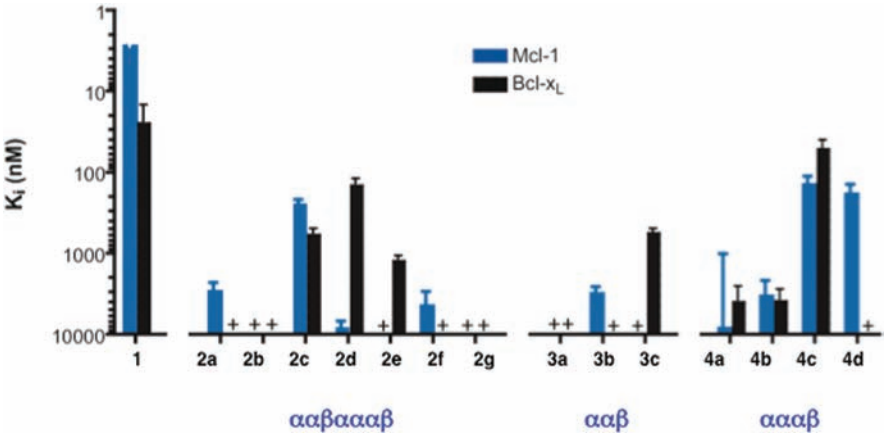

Figure 3. Graphical summary of inhibition constants (K_i) for binding to Mcl-1 (blue bars) or Bcl-x_L (black bars) for 18-mer α-peptide **1** and homologous α/β-peptides in families **2**−**4**, based on competition fluorescence polarization assays (see text for details). Note that the vertical axis is an inverse logarithmic scale, so that taller bars correspond to tighter binding (smaller K_i value, which should correspond to the K_d value).

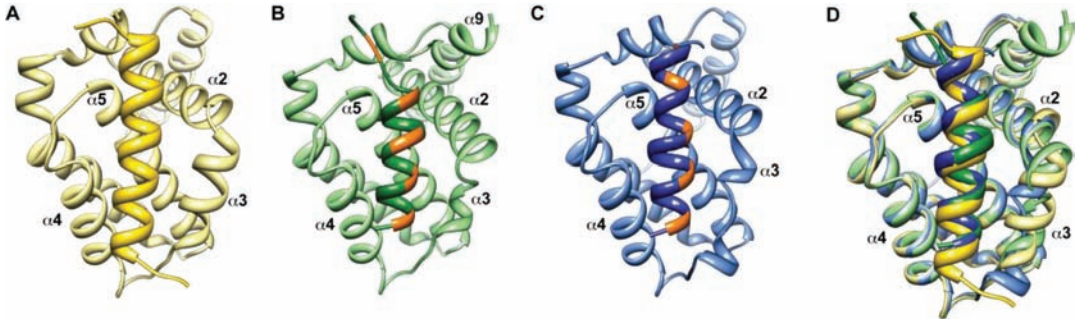

Figure 4. Crystal structures of α-peptide **5** (A; yellow; PDB: 3FDL[17]), α/β-peptide **2c** (B; green) and α/β-peptide **4c** (C; blue) bound to Bcl-x_L. In each case only the backbone is shown. The BH3 domain-derived peptides are indicated by the darker-colored helix at the center of each panel; the lighter-colored portions correspond to Bcl-x_L in each panel. For the two α/β-peptides, orange patches indicate the positions of the β^3-residues. Both α/β-peptides bind comparably to Bim BH3-derived α-peptide **5** in a groove formed predominantly by helices $\alpha2-\alpha5$ of Bcl-x_L. Part D shows an overlay of the three co-crystal structures, with colors as in parts A−C. Overall the structures are remarkably similar with the exception of the $\alpha3$ helix of Bcl-x_L.

conformations, depending on the identity of the bound ligand.[18] Indeed, two different conformations for $\alpha3$ are observed among the four copies of Bcl-x_L found in the asymmetric unit of the complex with α/β-peptide **4c** (only one of which is shown in C and D of Figure 4). In the **2c**:Bcl-x_L complex, helix $\alpha9$ is observed at the C-terminus of Bcl-x_L (Figure 4B), but no electron density is apparent for this helix in the other structures. Overall, the similarities among Bcl-x_L molecules in the various complexes suggest that it is reasonable to undertake detailed comparisons among the bound states of the Bim BH3 domain and the two different α/β-peptide analogues.

In both new structures the Bim-derived α/β-peptides make most or all of the expected side-chain contacts with Bcl-x_L, despite the multiple $\alpha \rightarrow \beta^3$ substitutions (Figures 4 and 5). BH3 domain sequences are defined by four hydrophobic residues (at positions conventionally designated h1−h4) in a pattern that causes the nonpolar side chains to become aligned upon α-helix formation.[11,19] In 18-mer α/β-peptide **2c**, h1−h4 are Ile3, Leu7, Ile10, and Phe14, respectively, while in **4c** these residues are Ile3, Leu7, β^3-hIle10, and β^3-hPhe14. In 26-mer α-peptide **5**, h1−h4 are Ile8, Leu12, Ile15, and Phe19. These four side chains of α-peptide **5** dock into complementary pockets along the floor of the BH3-recognition groove of Bcl-x_L, as is universally observed for BH3 domains bound to pro-survival proteins.[11] The h1−h4 side chains of α/β-peptide **2c** in the Bcl-x_L-bound structure align well with those of α-peptide **5**, and all four of these side chains from **2c** occupy the appropriate pockets on Bcl-x_L. α/β-Peptide **4c** differs from α-peptide **5** and α/β-peptide **2c** in that two of the key hydrophobic side chains are contributed by β^3-residues, β^3-hIle10 and β^3-hPhe14, while all four key side chains are contributed by α-residues of **5** and **2c**. Three of the four key hydrophobic side chains of α/β-peptide **4c**, those at positions h1, h2, and h4, overlay reasonably well with the analogous side chains of α-peptide **5** (Figure 5A). The h3 side chain of **4c** (β^3-hIle10; blue in Figure 5A), however, deviates somewhat from the corresponding Ile side chains of **5** and **2c** (Ile15 (yellow) and Ile10 (green), respectively); in contrast to the deep burial of the latter two side chains within the Bcl-x_L cleft, the β^3-hIle10 side chain of **4c** is only partially buried.

In addition to the characteristic set of hydrophobic side chains, a second defining feature of BH3 domains is an Asp residue located between h3 and h4.[11] Upon α-helix formation, the Asp side chain projects in a diametrically opposite direction relative to the h1−h4 stripe. Our structures of the **2c**:Bcl-x_L and **4c**:Bcl-x_L complexes reveal that the appropriate side-chain carboxylate (Asp12 in each case) forms a salt bridge with Arg139 on the

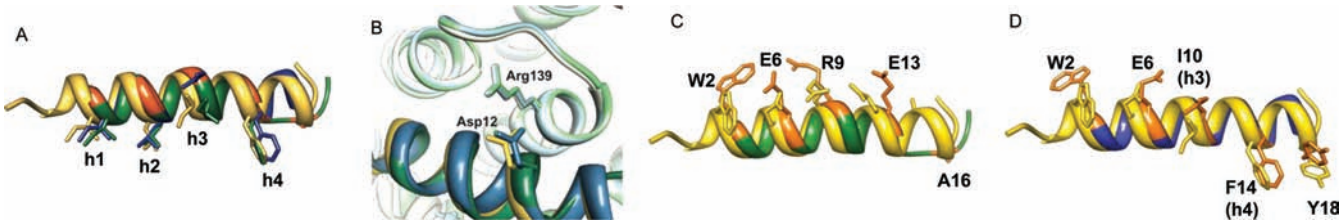

Figure 5. Overlay of α-peptide **5** (yellow), α/β-peptide **2c** (green), and α/β-peptide **4c** (blue) from the co-crystal structures shown in Figure 4. Part A highlights the positions of the h1−h4 side-chains. Part B highlights the intermolecular salt bridge between an Asp side chain on the outward-facing side of the α- or α/β-peptide and the Arg139 side chain from the Bcl-x_L. Parts C and D show pairwise comparisons of α/β-peptide **5** with either α/β-peptide **2c** (C) or α/β-peptide **4c** (D). These images compare the β^3-residue side chains of **2c** or **4c** with the corresponding α-residue side chains from **5**; these side chain sets display a consistent offset for **2c** (C) but not for **4c** (D) except for the Trp residue, as discussed in the text.

protein (Figure 5B), which matches the salt bridge observed in structures of authentic BH3 domain:antiapoptotic protein complexes such as **5**:Bcl-x_L.[17]

Overlay comparisons of each Bcl-x_L-bound α/β-peptide with Bim-derived α-peptide **5** are shown in part C (**2c** vs **5**) and part D (**4c** vs **5**) of Figure 5. In each case, the positions of the β^3-residues within each α/β-peptide are highlighted in orange, and in these images the β^3-residue side chains are orange as well (in contrast to Figure 5A). As anticipated, the $\alpha\alpha\beta\alpha\alpha\alpha\beta$ pattern of **2c** causes the β^3-residues to be aligned along one side of the helix (which faces away from Bcl-x_L; Figure 5C), while the α/β pattern of **4c** causes the β^3-residues to spiral around the helix periphery (Figure 5D). These images reveal unanticipated structural features. For **2c**, the positions of all β^3-residue side chains are spatially offset relative to the positions of the corresponding α-residue side chains in **5**. In contrast, for **4c** some of the β^3-residue side chains align fairly closely with the corresponding α-residue, particularly those at position 10 (h4) and position 14. We speculate that partial alignment in the case of **4c** arises because some β^3-residue side chains make intimate contact with Bcl-x_L. For **2c**, on the other hand, there is not a strong need for side-chain alignment, because in this case the β^3-residues, and their α-residue counterparts on **5**, project into the solvent.

The complex between α/β-peptide **2c** and Bcl-x_L displays one interesting difference relative to all complexes between BH3 domain α-peptides and pro-survival proteins: the α/β-peptide helix unwinds beyond Asn15. This C-terminal loss of helicity does not appear to be a consequence of crystal packing. The short nonhelical segment of **2c** includes one β^3-residue, β^3-hAla16, but any possible role of this unnatural subunit in the departure from helicity is impossible to determine by inspection of the crystal structure. The unusual conformation of the C-terminal segment of **2c** allows this portion of the α/β-peptide to make contacts with Bcl-x_L that have no parallels in other structures. For example, both β^3-hAla16 and Tyr18 make nonpolar contacts with the protein surface, and there is an H-bond between the side chains of Tyr17 from **2c** and Thr190 of the protein. It should be noted that comparable unwinding is *not* observed for α/β-peptide **4c**, which is fully helical in the Bcl-x_L-bound state. Nor is C-terminal helical unwinding observed in the recently reported crystal structure of a Puma-derived α/β-peptide bound to Bcl-x_L.[10b] The Puma-derived α/β-peptide has one additional C-terminal α-residue relative to **2c**, and the side-chain sequence is quite different from that of **2c**, but these two α/β-peptides have in common the $\alpha\alpha\beta\alpha\alpha\alpha\beta$ backbone pattern, the β^3-residue locations relative to the h1−h4 positions, and β^3-hAla as the β^3-residue nearest the C-terminus.

BH3 domain-derived α-peptides usually form very straight α-helices when bound to pro-survival proteins; for example, in the **5**:Bcl-x_L complex, the α-helix adopted by **5** has a 112 Å radius of curvature (a perfectly straight helix would have an infinite radius of curvature). α/β-Peptide **2c** shows a more pronounced (although still subtle) bowing of the helix, resulting in a 54 Å radius of curvature. This observation is consonant with our previous findings for a Puma-derived α/β-peptide that has an $\alpha\alpha\beta\alpha\alpha\alpha\beta$ backbone pattern analogous to that of **2c** (60 Å radius of curvature, averaged over two independent molecules in the crystal structure).[10b] In contrast, α/β-peptide **4c** forms a very straight helix when bound to Bcl-x_L (148 Å radius of curvature, averaged over four independent molecules in the crystal structure).

Despite the minor deviations from canonical BH3 α-peptide interactions with pro-survival proteins manifested by the BH3-derived α/β-peptides in the two new structures, i.e., the C-terminal helix unwinding observed for **2c** and the imperfect burial of the h3 side chain for **4c**, both of the new structures show that these α/β-peptides form a network of contacts with Bcl-x_L that mimics remarkably well those of the natural Bim BH3 domain. For **2c**, which has the $\alpha\alpha\beta\alpha\alpha\alpha\beta$ backbone pattern, this finding is consistent with structural data previously reported for a Puma-derived α/β-peptide.[10b] The β^3-residue placement in **2c** locates the β-stripe along the helix circumference between the stripe of h1−h4 side chains and the crucial Asp side chain. For **4c**, the mimicry of a natural BH3 domain is striking because the $\alpha\alpha\alpha\beta$ pattern causes the β^3-residues to spiral around the helix axis, and in the case of **4c** the h3 and h4 residues are derived from β^3-amino acids.

Global Analysis of $\alpha \rightarrow \beta$ Replacements. In the course of exploring various $\alpha \rightarrow \beta$ replacement patterns, we have placed a β^3-residue at each position of the Bim BH3 18-mer, and these replacements have occurred in different backbone contexts (i.e., different α/β patterns). We wondered whether global analysis of our set of α/β-peptide binding data might identify sequence positions at which $\alpha \rightarrow \beta$ replacement is either particularly favorable or particularly unfavorable in terms of binding to either Bcl-x_L or Mcl-1. Figure 6 provides a summary of binding results for each of the two protein targets, based on competition FP data. The α/β-peptides are grouped into two classes: weak binders and strong binders. The backbone pattern of each α/β-peptide is represented by a sequence of 18 blocks in which blue represents a β^3-residue (for binding to Bcl-x_L or Mcl-1, respectively), and white or green represents an α-residue.

The clearest pattern to emerge from this analysis is seen among the strong binders. For each target protein, several among the 18 positions are *never* occupied by a β^3-residue (green in Figure 6). For Bcl-x_L, $\alpha \rightarrow \beta$ replacement at positions 5, 8, 11, 12,

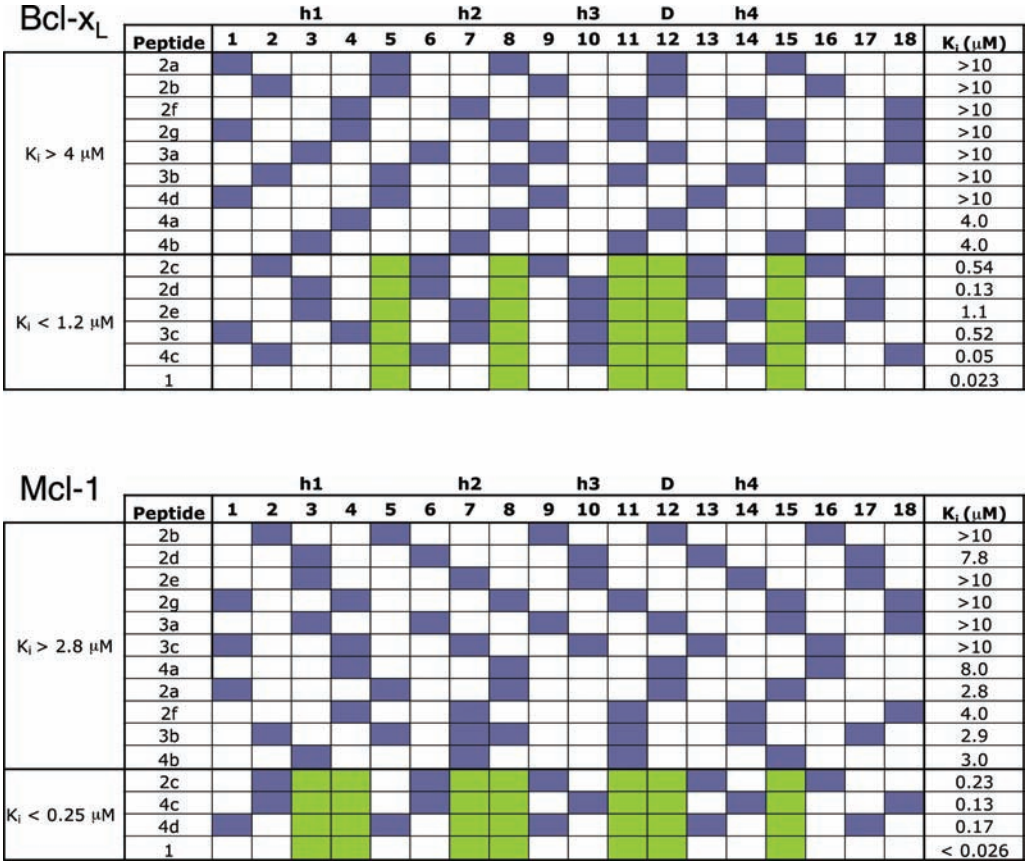

Figure 6. Global analysis of Bim BH3-derived α/β-peptide binding to Bcl-x_L (upper panel) or Mcl-1 (lower panel). The numbers across the top of each panel correspond to the sequence positions in the Bim-derived 18-mers introduced in this report (Figure 1). Five positions characteristic of BH3 domains, four hydrophobic residues (h1−h4), and an Asp residue (D) are indicated. The leftmost column of each panel classifies the α/β-peptides as strong or weak binders to the relevant pro-survival protein. The next column identifies each α- or α/β-peptide with number designations as in Figure 1. The remaining columns indicate whether the indicated position within the designated α/β-peptide is occupied by a β^3-residue (blue box) or by an α-residue (white or green box). The green boxes highlight positions in strong binders that appear to require an α-residue to form a complex with Bcl-x_L (upper panel) or with Mcl-1 (lower panel).

and 15 does not seem to be allowed for strong binding, and for Mcl-1 replacement at positions 3, 4, 7, 8, 11, 12, and 15 seems to be unfavorable. Although there is considerable overlap among the nonallowed positions for the two proteins (positions 8, 11, 12, and 15), our analysis identifies sequence positions that could be useful for design of protein-specific α/β-peptides. In particular, Bcl-x_L tolerates $\alpha \rightarrow \beta$ replacement at position 3 (the h1 site), position 4, and position 7 (the h2 site) among strong-binding α/β-peptides, but Mcl-1 does not appear to tolerate β^3-residues at these positions. On the other hand, Mcl-1 tolerates $\alpha \rightarrow \beta$ replacement at position 5 among strong binders, but Bcl-x_L does not. The pattern at h3 (position 10) is intriguing, because this position is occupied by a β^3-residue in four of six α/β-peptides that bind strongly to Bcl-x_L, while this position is an α-residue in all of the weak binders (of course, h3 is an α-residue in the Bim BH3 domain, which is a strong binder). In contrast, only one of the strong binders to Mcl-1 has a β^3-residue at the h3 position.

Rationalizing the pattern of $\alpha \rightarrow \beta$ tolerance in structural terms is challenging because we have structural data for only two Bim-derived α/β-peptides bound to Bcl-x_L and no structures for α/β-peptides bound to Mcl-1. The behavior at some positions can be tentatively tied to patterns that are broadly recognized among complexes between BH3 domains and pro-survival proteins. For example, position 12 corresponds to the highly conserved Asp that forms a salt bridge to the protein in many complexes (Figure 5),[11] and perturbing the carboxylate position is likely to be detrimental. Position 11 is a small residue (Ala or Gly) in most BH3 domains, and this residue occupies a sterically constrained region of the binding groove of pro-survival proteins. It therefore seems likely that this position would be very sensitive to even minor perturbations that arise from $\alpha \rightarrow \beta$ replacement. A similar argument would apply to substitutions at the h1 and h2 sites (positions 3 and 7),[11,14] which are apparently not allowed among tight binders to Mcl-1. Bcl-x_L, however, tolerates $\alpha \rightarrow \beta$ replacements at these critical positions, which may reflect a higher degree of flexibility in the binding groove of Bcl-x_L relative to Mcl-1.[18] All α/β-peptides with $\alpha \rightarrow \beta$ replacement at position 8 or 15 also have replacement at position 11 or 12; therefore, we cannot draw a firm conclusion about the intrinsic sensitivity of position 8 or 15 to replacement. Residues at these two positions are expected to be oriented toward solvent and not to engage in strong interactions with the partner protein; indeed, these positions in the Bim BH3 domain tolerate alanine mutations.[14] Therefore, we suspect that in the context of a different β^3-residue substitution pattern, positions 8 and 15 might ultimately be proven to tolerate $\alpha \rightarrow \beta$ replacement.

The trend at position 5 for binding to Bcl-x_L ($\alpha \rightarrow \beta$ replacement not allowed) is puzzling because this position is expected to be oriented toward solvent in the bound state. α/β-Peptide **4d**

dx.doi.org/10.1021/ja207148m | *J. Am. Chem. Soc.* 2012, 134, 315–323

Table 1. SPR Binding Data for α-Peptide 5 and α/β-Peptides 6, 7, 2c, and 4c

	IC_{50} (nM) [SPR][a]			
peptide	Bcl-x_L	Bcl-2	Bcl-w	Mcl-1
5	13 ± 4	41 ± 0.5	9 ± 0.5	1.1 ± 0.2
6	34 ± 6	98 ± 1	41 ± 13	1.7 ± 0.2
7	7.5 ± 2	5.2 ± 1	7.5 ± 0.5	2.4 ± 0.3
2c	1005 ± 25	4890 ± 370	620 ± 35	70 ± 7
4c	21 ± 1	107 ± 8	29 ± 2	109 ± 1

[a] Relative binding of α- and α/β-peptides to pro-survival proteins determined by competition assays using a Biacore instrument.

illustrates this puzzle, since this molecule has a β^3-residue at position 5 (but not at 8, 11, 12, or 15) and binds only weakly to Bcl-x_L; however, **4d** binds strongly to Mcl-1. It is possible that the effects of $\alpha \rightarrow \beta$ replacements on protein binding are cumulative, at least in some cases, and that rationalization based on purely local factors (as suggested in the previous paragraphs) will not always be possible. Despite this caveat, the analysis that emerges from Figure 6 offers a useful framework for future exploration of positional $\alpha \rightarrow \beta$ replacement tolerance within BH3 domain-derived α/β-peptides. In this regard, it is striking that a very similar pattern of $\alpha \rightarrow \beta$ replacement tolerance emerges when a comparable analysis is applied to smaller set of previously reported Puma-derived α/β-peptides[10a] (see Supplementary Figure S6, SI). Hence, it is possible that these trends provide general rules that could be applied to all BH3 sequence frameworks. Moreover, the similarity between trends among Puma- and Bim-derived α/β-peptides raises the intriguing possibility that particular binding profiles, either broad or selective among pro-survival proteins, could be achieved with irregular $\alpha \rightarrow \beta$ replacement patterns.

Extension of Selected α/β Patterns to 26-mer Length. Among Bim BH3-derived α-peptides, improvement in pro-survival protein binding profile is observed upon extension from 18-mer (**1**) to 26-mer (**5**).[11] We therefore examined the 26-mer α/β-peptides that correspond to **2c** and **4c**, i.e., **6** and **7**, respectively. In each case, the backbone pattern was maintained ($\alpha\alpha\beta\alpha\alpha\alpha\beta$ for **6**; $\alpha\alpha\alpha\beta$ for **7**), as was the native sequence of side chains (i.e., each β^3-residue in **6** or **7** is the homologue of the native α-residue). The 26-residue Bim BH3 α-peptide **5** is known to bind tightly to all pro-survival Bcl-2 family proteins.[14,16a] In our competition FP assays, we observed K_i < 3 nM for **5** binding to both Bcl-x_L and Mcl-1. We turned to competition surface plasmon resonance (SPR) measurements in order to compare **5** with 26-mer α/β-peptides **6** and **7** against a larger set of pro-survival proteins. The SPR data summarized in Table 1 show that **7** is the better of the two α/β-peptides in terms of reproducing the binding profile of the Bim BH3 domain (**5**). α/β-Peptide **7** shows comparable affinities for Bcl-2, Bcl-w, Bcl-x_L, and Mcl-1 relative to that of α-peptide **5**. In contrast, α/β-peptide **6** displays substantially weaker binding to Bcl-2, Bcl-w, and Bcl-x_L relative to that of α/β-peptide **5**, although **5** and **6** bind similarly to Mcl-1. SPR results are shown for 18-mers **2c** and **4c** for comparison with results for the 26-mers. Both 18-mers bind more weakly to each pro-survival protein than do the corresponding 26-mers (**6** and **7**, respectively). For Bcl-2, Bcl-w, and Bcl-x_L, **4c** binds significantly more tightly than does **2c**, in the SPR format.

We used mouse embryonic fibroblast (MEF) extracts (produced by permeabilising the plasma membrane with digitonin, leaving the mitochondrial membranes unaffected) to determine

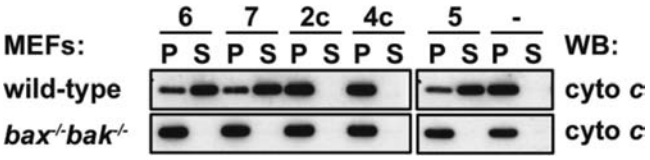

Figure 7. Cytochrome *c* release assay results. Permeabilised wild-type or $bax^{-/-}/bak^{-/-}$ mouse embryonic fibroblasts (MEFs) were treated with 26-mer Bim BH3 α-peptide **5**, homologous 26-mer α/β-peptide **6** or **7**, or 18-mer α/β-peptide **2c** or **4c**. All three of the 26-mer oligomers caused cytochrome *c* release from the pellet fraction (P), which contains mitochondria, into the soluble (S) cytosolic fraction of wild-type MEFs. No release was observed with 18-mer α/β-peptide **2c** or **4c**, which is consistent with their weaker affinity for pro-survival proteins, relative to 26-mers **5**−**7**. None of the peptides caused any cytochrome *c* release in $bax^{-/-}/bak^{-/-}$ MEFs.

Table 2. Proteolysis of α-Peptide 5 and α/β-Peptides 6 and 7

peptide	$t_{1/2}$ (min)[a]
5	≤0.1[b]
6	15
7	18

[a] Half-life of α- and α/β-peptides (10 μM) in the presence of proteinase K (10 μg/mL) in pH 7.5 TBS with 5% DMSO. Remaining peptide was graphed versus time and fit to a simple exponential decay equation to obtain a half-life in GraphPad Prism4. [b] α-Peptide **5** showed nearly complete degradation at the first time point (0.25 min); therefore, we provide an upper limit for the half-life.

whether α/β-peptides **6** and **7** can interact with the apoptosis signaling network; intact cells could not be employed in these studies because medium-length α/β-peptides typically do not cross membranes, as is also true for α-peptides of similar length. Wild-type MEFs are protected from apoptosis by both Mcl-1 and Bcl-x_L.[20] The Bim BH3 peptide **5** can induce apoptotic signaling, as manifested by release of cytochrome *c* from mitochondria in the MEF extracts (Figure 7). This behavior is expected since α-peptide **5** binds tightly to both Mcl-1 and Bcl-x_L, displacing pro-apoptotic proteins such as Bax or Bak that initiate the cascade of events leading to cytochrome *c* release. α/β-Peptides **6** and **7** were observed to induce cytochrome *c* release in wild-type MEF extracts (Figure 7), which is consistent with the SPR results showing tight binding to both Bcl-x_L and Mcl-1. Importantly, no release was observed following treatment of MEFs derived from $bax^{-/-}/bak^{-/-}$ mice, demonstrating that the activity of **6** and **7** in this assay depends on the expected signaling pathway. Neither of the18-mer α/β-peptides **2c** or **4c** induced cytochrome *c* release in MEF extracts, consistent with their relatively weak binding to Mcl-1 or Bcl-x_L observed via SPR (Table 1).

The use of unnatural oligomers to mimic signaling behavior of prototype α-peptides could be of therapeutic interest if the unnatural backbone resists biological degradation mechanisms. We used proteinase K to assess the susceptibility of α/β-peptides **6** and **7** to enzymatic cleavage. α-Peptide **5** is rapidly degraded under the conditions we employed ($t_{1/2} \leq 0.1$ min; Table 2), as expected. α/β-Peptides **6** and **7** displayed ≥150-fold stabilization relative to **5** toward proteinase K degradation. This result is consistent with previous findings for oligomers with the $\alpha\alpha\beta\alpha\alpha\alpha\beta$ backbone.[10a,12a] The resistance of **7** is noteworthy because of the $\alpha\alpha\alpha\beta$ backbone pattern; **7** contains one fewer β^3-residue than does **6**.

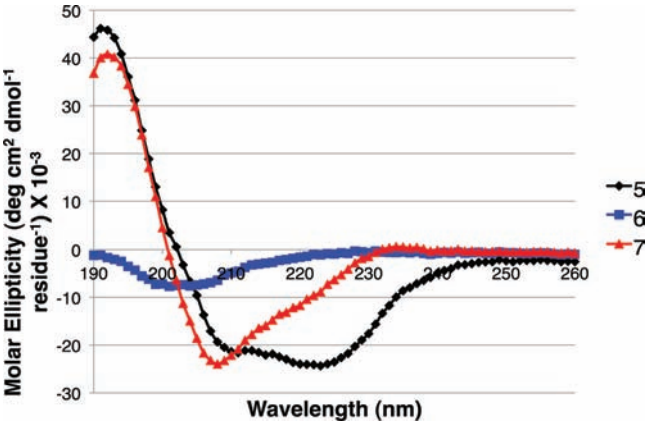

Figure 8. Circular dichroism data for 26-mer Bim BH3 α-peptide **5** and homologous 26-mer α/β-peptides **6** and **7** (25 μM peptide in 10 mM phosphate buffer, pH 7.5).

We have previously shown that formation of an α-helix-like conformation by α/β-peptides leads to a CD signature with a single minimum, near 205 nm.[8] A strong minimum in this region is observed for α/β-peptide **7**, but not for **6** (see Figure 8). Variable-concentration CD analysis (SI) suggests that **7** may self-associate under these conditions, while **6** appears not to self-associate. It is interesting that α/β-peptides **6** and **7** show similar levels of resistance to proteinase K degradation despite the apparent differences in helix-forming and/or self-association propensity.

CONCLUSIONS

We have used Bim BH3 domain mimicry as a model system to conduct comprehensive evaluation of oligomers with alternative α/β^3 arrangements. The most important outcome is our discovery that the $\alpha\alpha\alpha\beta$ pattern can provide functional mimicry of a signal-bearing α-helix while conferring significant resistance to proteolytic degradation. This finding expands the design horizon for α-helix-mimetic α/β-peptides, complementing previous work that highlighted the utility of the $\alpha\alpha\beta\alpha\alpha\alpha\beta$ pattern (this utility is reinforced by results provided here).[8,10,12] Our observations show that it is not necessary to confine β-amino acid residues within an α/β-peptide sequence to regions of the helical surface that make little or no contact with the partner protein.

The signaling properties of some BH3 domains have been effectively mimicked with orally bioavailable small molecules, which is a significant triumph in the realm of medicinal chemistry.[21] However, this achievement does not provide a basis for extending α-helix mimicry to longer examples that encompass more than four helical turns. In contrast, α/β-peptide design strategies are applicable to very long α-helical prototypes.[12] The results reported here expand the range of α/β combinations to be considered when one undertakes to mimic an informational α-helix.

EXPERIMENTAL PROCEDURES

General. Protected α-amino acids, resins, and 2-(1*H*-benzotriazole-1-yl)-1,1,3,3-tetramethyluronium hexafluorophosphate (HBTU) were purchased from Novabiochem. Protected β^3-homoamino acids were purchased from PepTech. 6-((4,4-Difluoro-1,3-dimethyl-5-(4-methoxyphenyl)-4-bora-3a,4a-diaza-s-indacene-2-propionyl)amino)hexanoic acid, succinimidyl ester (BODIPY-TMR-X-SE) was purchased from Invitrogen. All other reagents and solvents were purchased from Sigma Aldrich or Fisher and used as received. Reverse-phase HPLC was carried out on Vydac analytical or preparative-scale C18 columns using gradients between 0.1% TFA in water and 0.1% TFA in acetonitrile.

Peptide Synthesis and Purification. Peptides were synthesized using standard Fmoc solid-phase synthesis on Novasyn TGR resin or NovaPEG Rink amide resin. The primary synthesis of all peptides was performed in parallel in a fritted 96-well plate (Arctic white) at room temperature with a minimum coupling time of 1 h and deprotection time of 20 min. Microwave irradiation was used as previously described to repeat syntheses of selected α/β-peptides.[8b] Briefly, protected amino acids were activated with HBTU and *N*-hydroxybenzotriazole (HOBt) in the presence of *N*,*N*-diisopropylethylamine (DIEA) in NMP for coupling reactions. Deprotections were effected using 20% piperidine in DMF. After the final deprotection, peptides were capped using acetic anhydride/DIEA in DMF. Peptides **1** and **5** were synthesized using an Applied Biosystems Synergy 432A automated peptide synthesizer as previously described.[8b] After synthesis was complete, peptides were cleaved from the resin using a solution of 95% TFA, 2.5% H_2O, and 2.5% triisopropylsilane. Excess TFA was removed under a stream of nitrogen, and crude peptide was precipitated by addition of cold ether. Crude peptide solutions were purified using reverse-phase HPLC on preparative scale using C18 columns. The identity and purity of peptides were confirmed by MALDI-TOF-MS and analytical HPLC, respectively. After lyophilization, peptides were dissolved in DMSO, and concentration was determined by UV spectroscopy, based on the fact that each peptide contains two Tyr side chains and one Trp side chain (ε_{280} = 8250 cm^{-1} M^{-1}).[22] Fluorescently labeled peptides used as tracers in the competition and direct binding fluorescence polarization assays were synthesized as previously described.[15]

Protein Expression and Purification and Binding Measurements via FP. Expression and purification of Bcl-x_L and Mcl-1 were performed as previously described.[10a] Fluorescence polarization (FP) assays were conducted at room temperature in 384-well, nontreated, black polystyrene plates (Costar). Competitive and direct binding FP assays were conducted as reported previously.[10a] Briefly, for Bcl-x_L binding assays, the tracer used was the previously reported BODIPY^{TMR}-Bak tracer (previously reported dissociation constant (K_d) = 2.5 nM; however, we have more recently observed K_d = 1.2 nM).[10a] For Mcl-1 binding assays, the tracer used was the previously reported Flu-Bim tracer (K_d = 1.4 nM).[15] The K_d for tracer binding to pro-survival protein was remeasured with each new expression of protein and synthesis of tracer, and the resulting K_d value was used for calculation of inhibitor dissociation constant (K_i) values derived from that set of competition FP assays. Competition FP assays were conducted by adding 2 μL aliquots of serial dilutions of inhibitor in DMSO (final concentrations ranging from 4.2 pM to 25 μM) to 48 μL of tracer/protein mix in FP buffer (50 mM NaCl, 16.2 mM Na_2HPO_4, 3.8 mM KH_2PO_4, 0.15 mM NaN_3, 0.15 mM EDTA, 0.5 mg/mL Pluronic-F68, pH 7.5). For Bcl-x_L binding assays, the final concentrations of BODIPY^{TMR}-Bak tracer and Bcl-x_L were 3 nM and 2 nM, respectively. For Mcl-1 binding assays, the final concentrations of Flu-Bim tracer and Mcl-1 were 10 nM each. Experiments were performed in duplicate. After a 5 h incubation time, plates were analyzed on an Envision 2100 plate reader. The K_i value for each inhibitor was calculated as previously described using GraphPad Prism.[15]

Binding Measurements via SPR. Solution competition assays were performed using a Biacore 3000 instrument as described previously.[18] Briefly, pro-survival proteins (10 nM) were incubated with varying concentrations of peptide for at least 2 h in running buffer (10 mM HEPES, 150 mM NaCl, 3.4 mM EDTA, 0.005% (v/v) Tween 20, pH 7.4) prior to injection onto a CM5 sensor chip on which either a wild-type BimBH3 peptide or an inert BimBH3 mutant peptide (Bim4E) was immobilized. Specific binding of the pro-survival protein to the surface in the presence and absence of competitor α- or α/β-peptides was quantified by subtracting the signal obtained on the Bim mutant channel from that obtained on the wild-type Bim channel. The ability of the peptides to prevent protein

binding to immobilized BimBH3 was expressed as the IC_{50}, calculated by nonlinear curve fitting of the data with Kaleidagraph (Synergy Software).

Cytochrome *c* Release Assay. Mouse embryonic fibroblasts (wild-type, $bax^{-/-}/bak^{-/-}$) ($\sim 2 \times 10^6$ cells) were permeabilized in 20 mM HEPES pH 7.2, 100 mM KCl, 5 mM $MgCl_2$, 1 mM EDTA, 1 mM EGTA, 250 mM sucrose, 0.05% (w/v) digitonin (Calbiochem) supplemented with protease inhibitors (Roche), for 10 min on ice. The mitochondria-containing crude lysates were incubated with 10 μM peptide at 30 °C for 1 h before pelleting. The supernatant was retained as the soluble fraction, while the pellet, which contained intact mitochondria, was solubilized in 1% (v/v) Triton-X-100-containing lysis buffer (20 mM Tris-pH 7.4, 135 mM NaCl, 1.5 mM $MgCl_2$, 1 mM EDTA, 10% (v/v) glycerol) supplemented with protease inhibitors (Roche). Proteins were resolved by SDS-PAGE and transferred onto nitrocellulose membranes. Cytochrome *c* was detected with anti-cytochrome *c* antibody (7H8.2C12, BD Pharmingen).

Crystallization. We employed a "loop-deleted" form of human Bcl-x_L (Δ27−82 and without membrane anchor), which forms an α1 domain-swapped dimer yet retains BH3 domain binding activity.[17] Crystals were obtained by mixing Bcl-x_L with the appropriate α/β-peptide at a molar ratio of 1:1.3 and then concentrating the sample to 10 mg/mL. Crystals were grown by the sitting drop method at room temperature in 1.5 M ammonium sulfate, 0.1 M Tris pH 8.5, 12% (v/v) glycerol for **2c** or 25% (w/v) PEG 3350, 0.2 M lithium sulfate, 0.1 M Hepes pH 7.5 for **4c**. Prior to cryo-cooling in liquid N_2, crystals containing **4c** were equilibrated into cryoprotectant consisting of reservoir solution containing increasing concentrations of ethylene glycol to a final concentration of 15%. Crystals containing **2c** were mounted directly from the drop and plunge cooled in liquid N_2.

Diffraction Data Collection and Structure Determination. Diffraction data were collected at the Australian Synchrotron MX2 beamline. The diffraction data were integrated and scaled with XDS.[23] The structure was obtained by molecular replacement with PHASER[24] using the structure of Bcl-x_L from the Bim/Bcl-x_L complex (PDB: 3FDL), with the Bim peptide removed, as a search model. Several rounds of building in COOT[25] and refinement in PHENIX[26] led to the final model.

Proteolysis. Stock solutions of each peptide were prepared in a TBS solution with 10% DMSO (for solubility) at 100 μM as determined by UV absorbance. A 25 μg/mL stock solution of proteinase K was prepared in TBS. For each proteolysis reaction, 25 μL of peptide stock solution was mixed with 15 μL TBS. A 10 μL aliquot of proteinase K stock solution was added to the mixture, and the reaction was allowed to proceed at room temperature. A 100 μL aliquot of 1% TFA in 50:50 acetonitrile/H_2O was added to quench the reaction at the desired time point. A 125-μL aliquot of the resulting solution was injected onto an analytical reverse phase HPLC column, and the amount of full-length peptide remaining was quantified using the absorbance at 220 nm of this peptide. Duplicate reactions were run for each time point. Half-life values were determined by plotting the percent remaining peptide versus time and fitting the data to an exponential decay using GraphPad Prism. Amide bond cleavage sites were identified by MALDI-MS analysis of crude reaction mixtures at various time points.

Circular Dichroism (CD). All CD data were acquired using an Aviv 420 circular dichroism spectrophotometer. Peptide solutions were prepared in 10 mM phosphate buffer, pH 7.5, and the concentration was determined by UV absorbance. Data were acquired at 20 °C with a step value of 1 nm from 260 to 190 nm and an averaging time of 5.0 s. A 0.1-mm path length cell was used for all spectra. Signals were truncated to dynode voltages of <400 V.

■ ASSOCIATED CONTENT

Supporting Information. Supplementary Tables 1−3, supplementary Figures 1−7, further details of peptide characterization, and complete refs 6b and 21. This material is available free of charge via the Internet at http://pubs.acs.org.

■ AUTHOR INFORMATION

Corresponding Author
fairlie@wehi.edu.au; gellman@chem.wisc.edu

■ ACKNOWLEDGMENT

Research at UW-Madison was supported by NIH Grant R01 GM-056414. W.S.H. was supported in part by an NIH fellowship (CA119875), and K.J.K. was supported in part by the Chemistry-Biology Interface Training Program (T32GM008505). The CD instrument was purchased with a supplement to NIH grant R01 GM061238. In addition, this work was supported by fellowships and grants from Australian Research Council (Discovery Project Grant DP1093909 to W.D.F., P.M.C., B.J.S.), the NHMRC of Australia (Program Grant 461221 to P.M.C.), Australian Cancer Research Foundation (P.M.C.), and the Leukemia and Lymphoma Society (SCOR 7015-02) and an Australian Postgraduate Award (to O.B.C.). E.F.L. was supported by the Leukaemia Foundation of Australia (Phillip Desbrow Postdoctoral Fellowship). Crystallization trials were performed at the Bio21 Collaborative Crystallisation Centre. Data were collected on the MX2 beamline at the Australian Synchrotron, Victoria, Australia. Infrastructure support from NHMRC IRIISS Grant 361646 and the Victorian State Government OIS Grant is gratefully acknowledged.

■ REFERENCES

(1) (a) Jochim, A. L.; Arora, P. S. *Mol. Biosyst.* **2009**, *5*, 924. (b) Jochim, A. L.; Arora, P. S. *ACS Chem. Biol.* **2010**, *5*, 919. (c) Bullock, B. N.; Jochim, A. L.; Arora, P. S. *J. Am. Chem. Soc.* **2011**, *133*, 14220.

(2) (a) Guarracino, D. A.; Bullock, B. N.; Arora, P. S. *Biopolymers* **2011**, *95*, 1. (b) Guichard, G.; Huc, I. *Chem. Commun.* **2011**, *47*, 5933. (c) Goodman, C. M.; Choi, S.; Shandler., S.; DeGrado, W. F. *Nat. Chem. Biol.* **2007**, *3*, 252.(d) Hecht, S.; Huc, I.; Wiley-VCH, Wenheim, 2007. (e) Schafmeister, C. E.; Brown, Z. Z.; Gupta, S. *Acc. Chem. Res.* **2008**, *41*, 1387. (f) Davis, J.; Tsou, L.; Hamilton, A. *Chem. Soc. Rev.* **2006**, *36*, 326. (g) Yin, H.; Hamilton, A. D. *Angew. Chem., Int. Ed.* **2005**, *44*, 4130.

(3) (a) Werder, M.; Hauser, H.; Abele, S.; Seebach, D. *Helv. Chim. Acta* **1999**, *82*, 1774. (b) Kritzer, J. A.; Luedtke, N. W.; Harker, E. A.; Schepartz, A. *J. Am. Chem. Soc.* **2005**, *127*, 14584. (c) Stephens, O. M.; Kim, S.; Welch, B. D.; Hodsdon, M. E.; Kay, M. S.; Schepartz, A. *J. Am. Chem. Soc.* **2005**, *127*, 13126. (d) English, E. P.; Chumanov, R. S.; Gellman, S. H.; Compton, T. *J. Biol. Chem.* **2006**, *281*, 2661.

(4) (a) Hara, T.; Durell, S. R.; Myers, M. C.; Appella, D. H. *J. Am. Chem. Soc.* **2006**, *128*, 1995. (b) Hayashi, R.; Wang, D.; Hara, T.; Iera, J. A.; Durell, S. R.; Appella, D. H. *Bioorg. Med. Chem.* **2009**, *17*, 7884.

(5) (a) Ernst, J. T.; Kutzki, O.; Debnath, A. K.; Jiang, S.; Lu, H.; Hamilton, A. D. *Angew. Chem., Int. Ed.* **2002**, *41*, 278. (b) Kutzki, O.; Park, H. S.; Ernst, J. T.; Orner, B. P.; Yin, H.; Hamilton, A. D. *J. Am. Chem. Soc.* **2002**, *124*, 11838. (c) Ernst, J. T.; Becerril, J.; Park, H. S.; Yin, H.; Hamilton, A. D. *Angew. Chem., Int. Ed.* **2003**, *42*, 535. (d) Yin, H.; Lee, G. I.; Sedey, K. A.; Rodriguez, J. M.; Wang, H. G.; Sebti, S. M.; Hamilton, A. D. *J. Am. Chem. Soc.* **2005**, *127*, 5463. (e) Yin, H.; Lee, G. I.; Sedey, K. A.; Kutzki, O.; Park, H. S.; Orner, B. P.; Ernst, J. T.; Wang, H. G.; Sebti, S. M.; Hamilton, A. D. *J. Am. Chem. Soc.* **2005**, *127*, 10191. (f) Ahn, J.-M.; Han, S.-Y. *Tetrahedron Lett.* **2007**, *28*, 5343. (g) Hu, X.; Sun, J.; Wang, H.-G.; Manetsch, R. *J. Am. Chem. Soc.* **2008**, *130*, 13820. (h) Shaginian, A.; Whitby, L. R.; Hong, S.; Hwang, I.; Farooqi, B.; Searcey, M.; Chen, J.; Vogt, P. K.; Boger, D. L. *J. Am. Chem. Soc.* **2009**, *131*, 5564. (i) Campbell, F.; Plante, J. P.; Edwards, T. A.; Warriner, S. L.; Wilson, A. *J. Org. Biomol. Chem.* **2010**, *8*, 2344. (j) Lee, J. H.; Zhang, Q.; Jo, S.; Chai, S. C.; Oh, M.; Im, W.; Lu, H.; Lim, H.-S. *J. Am. Chem. Soc.* **2011**, *133*, 676.

(6) (a) Vassilev, L. T.; Vu, B. T.; Graves, B.; Carvajal, D.; Podlaski, F.; Filipovic, Z.; Kong, N.; Kammlott, U.; Lukacs, C.; Klein, C.; Fotohui, N.; Liu, E. A. *Science* **2004**, *303*, 844. (b) Oltersdorf, T.; et al. *Nature* **2005**,

435, 677. (c) Arkin, M. R.; Randal, M.; DeLano, W. L.; Hyde, J.; Luong, T. N.; Oslob, J. D.; Raphael, D. R.; Taylor, L.; Wang, J.; McDowell, R. S.; Wells, J. A.; Braisted, A. C. *Proc. Natl. Acad. Sci. U.S.A.* **2003**, *100*, 1603. (d) Ding, K.; Lu, Y.; Nikolovska-Coleska, Z.; Wang, G.; Qiu, S.; Shangary, S.; Gao, W.; Qin, D.; Stuckey, J.; Krajewski, K.; Roller, P. P.; Wang, S. *J. Med. Chem.* **2006**, *49*, 3432. (e) Buhrlage, S. J.; Bates, C. A.; Rowe, S. P.; Minter, A. R.; Brennan, B. B.; Majmudar, C. Y.; Wemmer, D. E.; Al-Hashimi, H.; Mapp, A. K. *ACS Chem. Biol.* **2009**, *4*, 335. (f) Fry, D. C. *Biopolymers* **2006**, *84*, 535. (g) Lessene, G.; Czabotar, P. E.; Colman, P. M. *Nat. Rev. Drug Discov.* **2008**, *7*, 989.

(7) (a) Walensky, L. D.; Kung, A. L.; Escher, I.; Malia, T. J.; Barbuto, S.; Wright, R. D.; Wagner, G.; Verdine, G. L.; Korsmeyer, S. J. *Science* **2004**, *305*, 1466. (b) Wang, D.; Liao, W.; Arora, P. S. *Angew. Chem., Int. Ed.* **2005**, *44*, 6525. (c) Wang, D.; Lu, M.; Arora, P. S. *Angew. Chem., Int. Ed.* **2008**, *47*, 1879. Henchey, L. K.; Porter, J. R.; Ghosh, I.; Arora, P. S. *ChemBioChem* **2010**, *11*, 2104. (d) Moellering, R. E.; Cornejo, M.; Davis, T. N.; Del Bianco, C.; Aster, J. C.; Blacklow, S. C.; Kung, A. L.; Gilliland, D. G.; Verdine, G. L.; Bradner, J. E. *Nature* **2009**, *462*, 182. (e) Stewart, M. L.; Fire, E.; Keating, A. E.; Walensky, A. E. *Nat. Chem. Biol.* **2010**, *6*, 595. (e) Bird, G. H.; Madani, N.; Perry, A. F.; Princiotto, A. M.; Supko, J. G.; He, X. Y.; Gavathiotis, E.; Sodroski, J. G.; Walensky, L. D. *Proc. Natl. Acad. Sci. U.S.A.* **2010**, *107*, 14093.

(8) (a) Horne, W. S.; Price, J. L.; Keck, J. L.; Gellman, S. H. *J. Am. Chem. Soc.* **2007**, *129*, 4178. (b) Horne, W. S.; Price, J. L.; Gellman, S. H. *Proc. Natl. Acad. Sci. U.S.A.* **2008**, *105*, 9151. (c) Giuliano, M. W.; Horne, W. S.; Gellman, S. H. *J. Am. Chem. Soc.* **2009**, *131*, 9860. (d) Price, J. L.; Horne, W. S.; Gellman, S. H. *J. Am. Chem. Soc.* **2010**, *132*, 12378.

(9) Steer, D. L.; Lew, R. A.; Perlmutter, P.; Smith, A. I.; Aguilar, M. I. *Curr. Med. Chem.* **2002**, *9*, 811.

(10) (a) Horne, W. S.; Boersma, M. D.; Windsor, M. A.; Gellman, S. H. *Angew. Chem., Int. Ed.* **2008**, *47*, 2853. (b) Lee, E. F.; Smith, B. J.; Horne, W. S.; Mayer, K. N.; Evangelista, M.; Colman, P. M.; Gellman, S. H.; Fairlie, W. D. *ChemBioChem* **2011**, *12*, 2025.

(11) (a) Sattler, M.; Liang, H.; Nettesheim, D.; Meadows, R. P.; Harlan, J. E.; Eberstadt, M.; Yoon, H. S.; Shuker, S. B.; Chang, B. S.; Minn, A. J.; Thompson, C. B.; Fesik, S. W. *Science* **1997**, *275*, 983. (b) Petros, A. M.; Nettesheim, D. G.; Wang, Y.; Olejniczak, E. T.; Meadows, R. P.; Mack, J.; Swift, K.; Matayoshi, E. D.; Zhang, H.; Thompson, C. B.; Fesik, S. W. *Protein Sci.* **2000**, *9*, 2528. (c) Smits, C.; Czabotar, P. E.; Hinds, M. G.; Day, C. L. *Structure* **2008**, *16*, 818. (d) Liu, X.; Dai, S.; Zhu, Y.; Marrack, P.; Kappler, J. W. *Immunity* **2003**, *19*, 341. (e) Czabotar, P. E.; Lee, E. F.; van Delft, M. F.; Day, C. L.; Smith, B. J.; Huang, D. C.; Fairlie, W. D.; Hinds, M. G.; Colman, P. M. *Proc. Natl. Acad. Sci. U.S.A.* **2007**, *104*, 6217.

(12) (a) Horne, W. S.; Johnson, L. M.; Ketas, T. J.; Klasse, P. J.; Lu, M.; Moore, J. P.; Gellman, S. H. *Proc. Natl. Acad. Sci. U.S.A.* **2009**, *106*, 14751. (b) Johnson, L. M.; Horne, W. S.; Gellman, S. H. *J. Am. Chem. Soc.* **2011**, *133*, 10038.

(13) Harbury, P. B.; Zhang, T.; Kim, P. S.; Alber, T. *Science* **1993**, *262*, 1401.

(14) Lee, E. F.; Czabotar, P. E.; van Delft, M. F.; Michalak, E. M.; Boyle, M. J.; Willis, S. N.; Puthalakath, H.; Bouillet, P.; Colman, P. M.; Huang, D. C.; Fairlie, W. D. *J. Cell. Biol.* **2008**, *180*, 341.

(15) Boersma, M. D.; Sadowsky, J. D.; Tomita, Y. A.; Gellman, S. H. *Protein Sci.* **2008**, *17*, 1232.

(16) (a) Chen, L.; Willis, S. N.; Wei, A.; Smith, B. J.; Fletcher, J. I.; Hinds, M. G.; Colman, P. M.; Day, C. L.; Adams, J. M.; Huang, D. C. *Mol. Cell* **2005**, *17*, 393. (b) Certo, M.; Del Gaizo Moore, V.; Nishino, M.; Wei, G.; Korsmeyer, S.; Armstrong, S. A.; Letai, A. *Cancer Cell* **2006**, *9*, 351. (c) Ku, B.; Liang, C.; Jung, J. U.; Oh, B. H. *Cell Res* **2011**, *21*, 627.

(17) Lee, E. F.; Sadowsky, J. D.; Smith, B. J.; Czabotar, P. E.; Peterson-Kaufman, K. J.; Colman, P. M.; Gellman, S. H.; Fairlie, W. D. *Angew. Chem., Int. Ed.* **2009**, *48*, 4318.

(18) Lee, E. F.; Czabotar, P. E.; Yang, H.; Sleebs, B. E.; Lessene, G.; Colman, P. M.; Smith, B. J.; Fairlie, W. D. *J. Biol. Chem.* **2009**, *284*, 30508.

(19) Kelekar, A.; Thompson, C. B. *Trends Cell. Biol.* **1998**, *8*, 324.

(20) Willis, S. N.; Chen, L.; Dewson, G.; Wei, A.; Naik, E.; Fletcher, J. I.; Adams, J. M.; Huang, D. C. *Genes Dev.* **2005**, *19*, 1294.

(21) Park, C. -M.; et al. *J. Med. Chem.* **2008**, *51*, 6902.

(22) Gill, S. C.; von Hippel, P. H. *Anal. Biochem.* **1989**, *182*, 319.

(23) Kabsch, W. *Acta Crystallogr., Sect. D* **2010**, *66*, 125.

(24) (a) McCoy, A. J.; Grosse-Kunstleve, R. W.; Storoni, L. C.; Read, R. J. *Acta Crystallogr., Sect. D* **2005**, *61*, 458. (b) Read, R. J. *Acta Crystallogr., Sect. D* **2001**, *57*, 1373. (c) Storoni, L. C.; McCoy, A. J.; Read, R. J. *Acta Crystallogr., Sect. D* **2004**, *60*, 432.

(25) Emsley, P.; Cowtan, K. *Acta Crystallogr., Sect. D* **2004**, *60*, 2126.

(26) Adams, P. D.; Grosse-Kunstleve, R. W.; Hung, L. W.; Ioerger, T. R.; McCoy, A. J.; Moriarty, N. W.; Read, R. J.; Sacchettini, J. C.; Sauter, N. K.; Terwilliger, T. C. *Acta Crystallogr., Sect. D* **2002**, *58*, 1948.